Emission spectroscopy of long pulse relativistic electron-beam-produced argon plasmas

M. L. Brake, T. Repetti, K. Pearce, and R. Lucey
Department of Nuclear Engineering, University of Michigan, Ann Arbor, Michigan 48109

(Received 19 December 1985; accepted for publication 12 March 1986)

Visible emission spectroscopy of long pulse, relativistic, electron-beam (300 ns, 1 kA, 300 keV)-produced argon plasmas has been performed over a wide pressure range (1–750 Torr). The emission spectra were observed between 350 and 600 nm with a spectrograph coupled to an optical multichannel analyzer, which was gated with pulses of 50 and 500 ns. Singly ionized argon lines were observed at all pressures and all times during the beam current. The relative line intensities for the $(4s\text{–}4p)$ transitions fit those described by an equilibrium distribution at approximately 2 eV. The emission lines originating from the higher excited states of $(4s'\text{–}4p')$ and $(4s''\text{–}4p'')$ were much larger than expected in a 2-eV plasma, and this enhancement can be attributed to the presence of the beam electrons.

INTRODUCTION

Emission spectroscopy has been used to study plasmas produced by short pulse electron beam accelerators[1–5] (3–40 ns) for both low and high (> 1 atm) pressures. The light produced by electron beams is of particular interest since *e*-beam devices are potential pump sources for excimer lasers,[6] nitrogen lasers,[7] and vacuum ultraviolet (VUV) lasers.[8] Due to diode closure and the rarity of long pulse electron beam accelerators, little research has been performed on plasmas produced by long pulse *e*-beam interactions, nor have many studies examined the intermediate pressure range of 1–750 Torr. In this paper we report the results of spectroscopic measurements of argon plasmas produced by *e*-beam pulse lengths of about 300 ns injected into argon pressures, ranging from 1 to 750 Torr.

Many researchers have felt that the visible emission produced by electron beams is dominated by atomic collisions with the secondary electrons which are produced by impact ionization by the beam electrons.[9] Recently there has been a theory proposed by Jayakumar and Fleischmann[10] that predicts that the presence of fast particles can significantly enhance allowed radiative transitions, particularly those from highly excited states, and that it is the fast particles and not the secondary electrons that dominate this effect. As will be shown in this paper, this theory seems to describe the results of our experiments quite well.

EXPERIMENT

The experimental configuration (see Fig. 1) consisted of a Febetron, relativistic electron beam accelerator, with long pulse modules. The diode consisted of a 2.5-cm-diam carbon brush cathode and a 0.025-mm titanium anode foil. The electron beam had a peak current of 1 kA, a peak voltage of 300 kV, and a pulse length of about 300 ns (see Fig. 2). The beam current was measured with a calibrated pickup loop placed near the diode on the cathode side of the foil. The beam voltage was measured with a thin-film capacitive probe sensing the region between the marx bank and the cathode stalk. The electron beam was injected into an aluminum vacuum vessel which had plexiglass windows on the sides and end. The emitted light at several argon pressures (1–750 Torr) was examined. The light was analyzed by a 0.275-m spectrograph coupled to an optical multichannel analyzer (OMA). The spectrograph contained two gratings: a 1200-grooves/mm grating, with about 75-nm dispersion over the length of the detector (2.54 cm), and a 600-grooves/mm grating, with about 150-nm dispersion over the length of the detector. The OMA was gated with pulses of 50 and 500 ns. Light was examined both radially and axially, although the light intensity in the radial direction was too low to be detected in these experiments. The scattering of the electrons through the titanium foil resulted in the beam spreading out into a cone of 80°.[11] Thus the plasma was brightest closest to the foil, and the optics gathered light from this region to obtain the best possible signal-to-noise ratio. Emission spectra obtained with the optics focused several centimeters from the foil were identical to the spectra

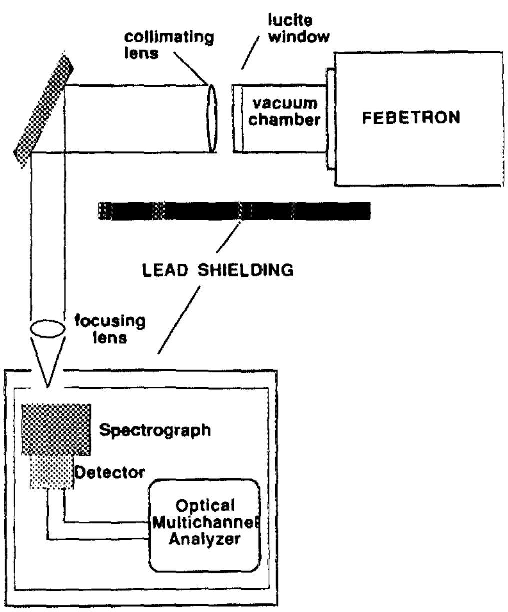

FIG. 1. Experimental configuration.

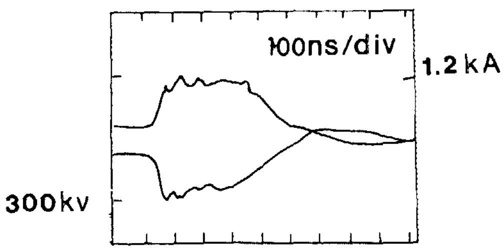

FIG. 2. Oscilloscope trace of the electron beam current (top trace) and the voltage (bottom trace).

obtained near the foil, except that the intensity was greatly reduced. It is assumed that the majority of the emission spectra presented here came from plasma close to the foil.

RESULTS

Time histories of the argon emission spectra were taken by gating the OMA with pulses 50 ns long and moving the delay of the gate pulse by 50 ns, with respect to the rise of the beam current, for pressures of 12 and 100 Torr. These spectra were obtained using the 1200-grooves/mm grating and the lines were calibrated by means of a krypton calibration lamp and tables of known lines.[12] A pressure history of the argon emission spectra was obtained using the 600-grooves/mm grating, by examining time integrated shots (gates of 500 ns) for pressures ranging from 1 to 750 Torr (see Fig. 3). In all cases, all of the emission lines were identified as originating from allowed transitions in singly ionized argon ions. No light emission was detected after the beam current had returned to zero.

The relative intensities of several ion lines were used to estimate the plasma temperature. The line intensities were adjusted for the spectral response of the optical system by calibrating the optical system with a tungsten filament lamp. The lines used were 438.4, 448.2, 454.5, 461.0, 465.8, 473.6, and 476.5 nm, the majority of which are $4s$–$4p$ transitions[17] (see Fig. 4). An atomic Boltzmann plot was used to determine the temperatures[13] (see Fig. 5). This method assumes that the plasma is in local thermodynamic equilibrium (LTE) and that the spectral lines are not affected by self-absorption. The atomic Boltzmann plot is obtained by plotting $\ln(I\lambda/gA)$ as a function of E_m, where I is the intensity of the line (corrected for the spectral response of the optics), λ is the wavelength, g is the degeneracy of the upper level, A is the transition probability of the upper level, and E_m is the energy of the upper level. The negative inverse slope of the line is taken as the temperature. The g and A constants are found in Ref. 14. The fit of the points to a straight line is taken as the existence of local thermodynamic equilibrium. The measured temperature was beteween 1.6 and 2.4 eV ($\pm$ 1.0 eV) and stayed about the same for all times and all pressures. This is consistent with the fact that the intensities are dominated by the fast particles and the current is relatively flat for about 250 ns (see Fig. 2).

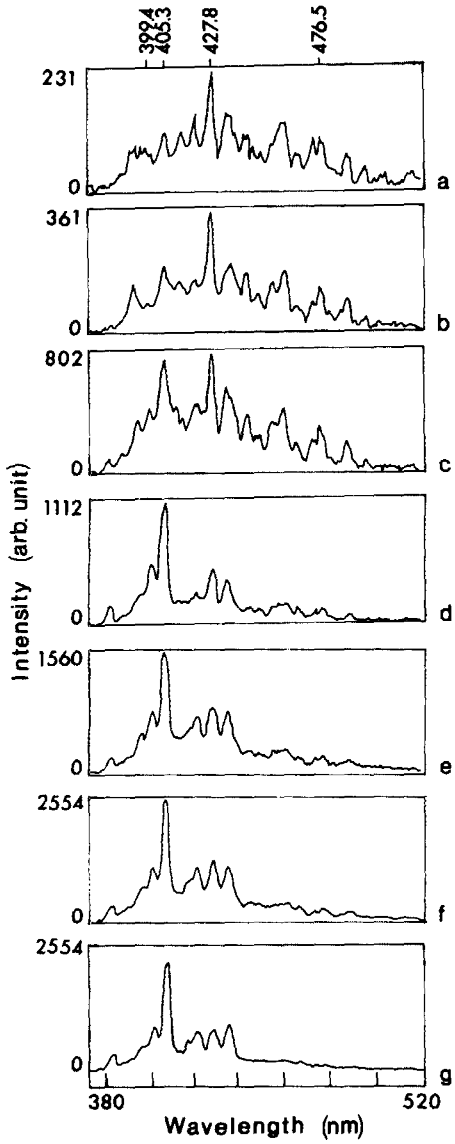

FIG. 3. Time-integrated emission spectra (500-ns gates) for several argon pressures: (a) 1 Torr, (b) 12 Torr, (c) 50 Torr, (d) 100 Torr, (e) 200 Torr, (f) 380 Torr, (g) 750 Torr.

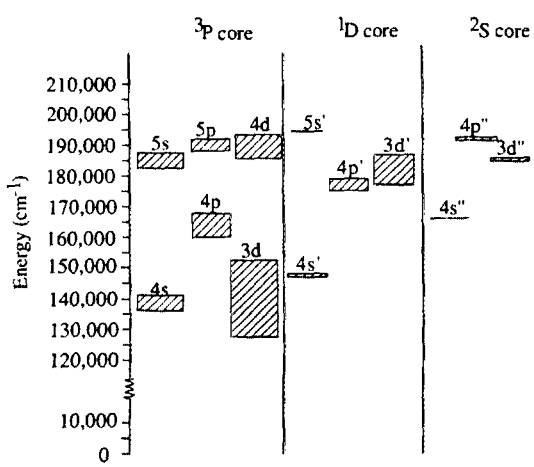

FIG. 4. Energy level diagram for Ar^+ constructed from data of Ref. 17.

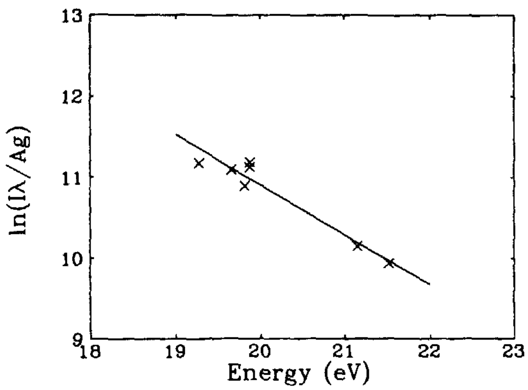

FIG. 5. Atomic Boltzmann plot for argon at 1 Torr pressure. The inverse of the slope gives a temperature of 1.6 eV.

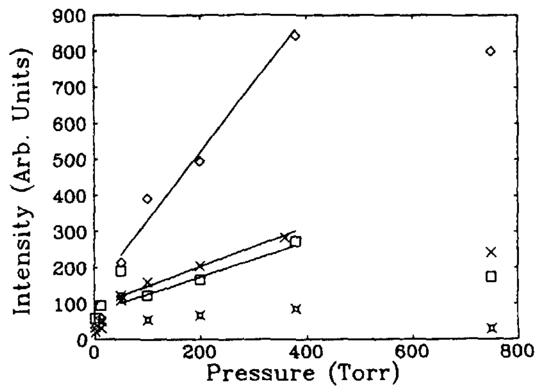

FIG. 6. Intensity of argon ion emission lines for the transitions $4s''$–$4p''$ at 405.3 nm (◈) and 399.5 nm (×), for the $4s'$–$4p'$ at 427.8 nm (□), and for the $4s$–$4p$ at 476.5 nm (⌑) as a function of argon gas pressure.

DISCUSSION

When an electron beam is injected into a neutral gas, the energetic beam electrons ionize and excite the gas atoms. Before the density of ions reaches the value needed for space-charge neutralization, there exists a large radial electric field which results in the loss of all of the secondary electrons to the walls. Once charge neutralization has occurred, the axial electric field dominates and the secondary electron density can increase. (This charge neutralization occurs in a few nanoseconds or less for the experimental conditions described here.) These secondary electrons produced by beam ionization further ionize and excite the gas. These secondary electrons become thermalized by the balance of energy gain from resistive heating from the plasma return currents and energy loss due to ionization and excitation. Note it is very difficult to distinguish the secondary electrons from the thermal electrons.

The thermalized plasma can last for some time after the electron beam. The was the case for Ono[5,9] and Rizzo[3,15] who observed emission spectra anywhere from a few tens of nanoseconds to microseconds after the beam current had returned to zero. In the experiment described here, emission spectra were only observed during the beam current. Ono[5,9] and Rizzo[3,15] used higher current and higher energy beams than this experiment, however (10 kA, 600 keV and 37 kA, 1.5 MeV, respectively). Light emission after the beam current indicates that the collisional processes of Ono's[5,9] and Rizzo's[3,15] plasmas were dominated by the secondary and thermal electrons produced by the beam ionization. For this experiment, the beam electrons played a more dominant role in the collisional processes. This result is illustrated by the fact that the light emission was no longer detectable after the beam current had ended (the plasma electron density after the current had ended was not large enough to produce enough excitations needed to produce detectable emission spectra), and the fact that the intensity of the line emission and thus the plasma temperature determined from the spectra remained constant for the flat part of the beam current, about 250 ns. Since it is difficult to measure the plasma electron density, we cannot qualitatively compare the effect of the beam electrons on ionization processes to the effect of the thermal electrons on ionization processes.

Ono[5,9] observed two high-intensity spectral lines in a singly ionized electron beam produced argon plasma at 351.0 and 427.8 nm. He concludes that these lines are "self-terminating laser lines." The pulse width of Ono's electron beam accelerator was 3 ns and the width of his "laser lines" were also about 3 ns, although the time resolution of his system made it difficult to determine the pulse width exactly. We also observe a high-intensity spectral line at 427.8 nm as well as 399.5 and 405.3 nm. As mentioned above, the current from our beam remained flat for about 250 ns and the intensity of these intense lines also remained constant for the entire duration of the beam, and then disappeared when the beam current returned to zero. Thus, this longer pulse has made it possible for us to show that these "laser lines" are directly related to the beam current and thus the beam electrons. This is substantiated by the fact that the light emission increased linearly as the pressure was increased (see Fig. 6) for the region of about 50–380 Torr. If these lines were pumped by secondary or thermal electrons, then the intensity should increase as the square of the pressure or a more complicated power because the thermal and secondary electrons are at least a linear function of the pressure for a singly ionized gas. That is, if the laser lines were pumped by the following reaction,

$$A + e_{\text{thermal}} \rightarrow A^{+}(\text{excited}) + 2e, \qquad (1)$$

then the population of the upper state of the laser line would follow

$$dN_{\text{upper}}/dt = K[A][n_p], \qquad (2)$$

where n_p is the density of the secondary and thermal electrons and K is the rate constant determined from the cross section for ionization and excitation. On the other hand, if the beam electrons pump the upper state by the following reaction,

$$A + e_{\text{beam}} \rightarrow A^{+}(\text{excited}) + 2e, \qquad (3)$$

then the population of the laser line would follow,

$$dN_{\text{upper}}/dt = K[A][n_{\text{beam}}], \qquad (4)$$

which depends linearly upon the pressure, because the beam density does not depend upon the pressure. (The beam is spread out by the foil, and this does not depend upon pres-

TABLE I. Atomic data for 399.4, 405.3, 427.8, and 476.5 nm.[14]

Wavelength (nm)	Energy of upper state (cm^{-1})	Degeneracy of upper state	Transition probability ($10^8\ s^{-1}$)
399.4	192333	2	1.6
405.3	191975	4	1.5
427.8	172214	4	1.0
476.5	160239	4	0.575

sure when examining light close to the foil.) Note that as the pressure increases to 750 Torr, recombination processes become increasingly important, resulting in depopulation of excited states before they have had the chance to radiate.

Another interesting result of the data presented here is that these large intensity lines originate from high-energy states, specifically the transition of the $4s'$–$4p'$ at 427.8 nm and the two transitions of the $4s''$–$4p''$ at 399.4 and 405.3 nm (see Table I and Fig. 4). The intensities observed at these wavelengths are much larger than would be expected of a plasma in equilibrium at a temperature of approximately 2 eV. As will be shown below, this enhancement of upper level transitions can be attributed to the effects of the fast (beam) particles.

In a recent paper, Jayakumar and Fleischmann[10] proposed that "allowed transitions are significantly enhanced in the presence of fast particles without significantly enhancing the corresponding deexcitation rates" and even though the "limiting conditions for LTE are nearly unaltered, the populations of highly excited states are enhanced." They claim that even small densities of fast particles may result in significant effects. They show that in a two-level system, the excited state population is enhanced proportional to the enhancement of the excitation rate by the fast particles. This enhancement can be expressed as follows:

$$\xi_m = 1 + (n_f/n_p)F_{0m}\xi \exp(E_m/T_e), \tag{5}$$

where n_f is the density of the fast (beam) particles, n_p is the density of the plasma (thermal) electrons, ξ is a constant (of 1 for allowed transitions), E_m is the energy of the upper state, T_e is the electron temperature, and F_{0m} is a parameter which relates the ratio of the fast particle-induced rates to the corresponding rates for plasma electrons and is given by

$$F_{0m} = 7\times 10^{-3}\, T_e^{1/2} Z^2/G \tag{6}$$

for relativistic particles, where Z is the charge of the fast particle and G is the Gaunt factor, usually about 0.2 for ions.[16] Thus the relative population density of an upper state to the ground state is

$$n_m/n_0 = \xi_m (g_m/g_0)\exp(-E_m/T_e), \tag{7}$$

where g_m and g_0 are the degeneracy factors. This relation was used to compare the enhancement of the $4s'$–$4p'$ and $4s''$–$4p''$ transitions relative to the $4s$–$4p$ transitions.

For the conditions of this experiment, the beam density was approximately 10^{11} cm^{-3}. We assume 10^{14} cm^{-3} to be an upper bound on the plasma density (based upon the fact that Rizzo[3,15] who had a much more intense beam than ours measured a plasma density of about 10^{16} cm^{-3}). Using these values predicts that $(n_f/n_p)F_{0m}\xi \exp(E_m/T_e)$ is of the order 40 to 500 depending upon the line of interest. We will also assume that the excited states are directly excited by the beam electrons, making them an effective two-level system. Using the above equations and the fact that $1 \ll (n_f n_p)F_{0m}\xi \exp(E_m/T_e)$ and $\xi = 1$, the intensity of one spectral line compared to another can be written as

$$\frac{I'}{I} = \left(\frac{I'}{I}\right)_{\rm LTE} \frac{\zeta'}{\zeta}, \tag{8}$$

where

$$\frac{\zeta'}{\zeta} = \exp\frac{(E'_m - E_m)}{T_e}, \tag{9}$$

where E'_m and E_m are the upper energy level of the transition for the primed and unprimed spectral lines and

$$\left(\frac{I'}{I}\right)_{\rm LTE} = \frac{A'g'\lambda}{Ag\lambda'} \exp\frac{-(E'_m - E_m)}{kT_e}, \tag{10}$$

where A is the transition probability and g is the degeneracy of the upper state. This calculation has been performed for the three highly excited transitions (399.5, 405.2, and 427.8 nm) relative to the transition at 476.5 nm (see Tables II, III, and IV). Henceforth, the primed intensities denote intensities originating from the highly excited states and the unprimed intensity will denote the intensity of the $4s$–$4p$ transition at 476.5 nm. The first column in Tables II, III, and IV

TABLE II. The ratio of the measured intensity of the 399.5-nm line to the 476.5-nm line, $(I'/I)_{\rm exp}$, the ratio as determined by LTE at a temperature of 2 eV, $(I'/I)_{\rm LTE}$, the amount of measured enhancement, $(I'/I)_{\rm exp}/(I'/I)_{\rm LTE}$, and the degree of enhancement predicted by theory (ζ'/ζ).

Pressure (Torr)	$(I'/I)_{\rm exp}$	$(I'/I)_{\rm LTE}$	$\frac{(I'/I)_{\rm exp}}{(I'/I)_{\rm LTE}}$	(ζ'/ζ)
50	0.90	0.23	4.0	7.3
100	3.00	0.23	13.0	7.3
200	3.07	0.23	13.3	7.3
380	3.37	0.23	14.7	7.3

TABLE III. The ratio of the measured intensity of the 405.3-nm line to the 476.5-nm line, $(I'/I)_{\rm exp}$, the ratio as determined by LTE at a temperature of 2 eV, $(I'/I)_{\rm LTE}$, the amount of measured enhancement, $(I'/I)_{\rm exp}/(I'/I)_{\rm LTE}$, and the degree of enhancement predicted by theory (ζ'/ζ).

Pressure (Torr)	$(I'/I)_{\rm exp}$	$(I'/I)_{\rm LTE}$	$\frac{(I'/I)_{\rm exp}}{(I'/I)_{\rm LTE}}$	(ζ'/ζ)
50	1.76	0.43	4.1	7.2
100	7.26	0.43	16.9	7.2
200	7.40	0.43	17.2	7.2
380	10.04	0.43	23.3	7.2

TABLE IV. The ratio of the measured intensity of the 427.8-nm line to the 476.5-nm line, $(I'/I)_{exp}$, the ratio as determined by LTE at a temperature of 2 eV, $(I'/I)_{LTE}$, the amount of measured enhancement, $(I'/I)_{exp}/(I'/I)_{LTE}$, and the degree of enhancement predicted by theory (ζ'/ζ).

Pressure (Torr)	$(I'/I)_{exp}$	$(I'/I)_{LTE}$	$\frac{(I'/I)_{exp}}{(I'/I)_{LTE}}$	(ζ'/ζ)
50	1.56	0.92	1.7	2.1
100	2.28	0.92	2.5	2.1
200	2.48	0.92	2.7	2.1
380	3.25	0.92	3.5	2.1

gives the ratio of the measured intensity of the line in question to the intensity of the line at 476.5 nm, $(I'/I)_{exp}$, the second column gives the ratio of the two intensities as determined from equilibrium considerations at a temperature of 2 eV, $(I'/I)_{LTE}$, the third column gives the ratio of column one to column two, i.e., the measured amount of enhancement, $(I'/I)_{exp}/(I'/I)_{LTE}$, and column four gives the amount of enhancement as determined from Eq. (9) (ζ'/ζ). Note that the experimentally determined enhancement shows a slight pressure dependence, whereas the theoretical enhancement does not have any different pressures. Also, a careful measurement of the plasma density needs to be made so that the approximations and regions of validity involved in the theory of Jayakumar and Fleischmann[10] can be confirmed. Nonetheless, considering the assumptions involved, the uncertainties in the transition probabilities (as great as 50%), and the uncertainties in the measured temperatures, the theoretically predicted enhancement matches the measured enhancement reasonably well.

CONCLUSIONS

For long pulse (300 ns) electron-beam-produced argon plasmas, the emission spectrum results in singly ionized lines for all times, with the disappearance of these lines occurring simultaneously with the beam turn off. The plasma temperatures as determined from atomic Boltzmann plots are about 2 eV regardless of when they are measured in time relative to the beam current and regardless of pressure, over the range of 1–750 Torr. The collisional dynamics of the plasma are dominated by the beam electrons for pressures between 50 and 380 Torr. The lines which originate from highly excited states are enhanced due to the presence of the fast beam electrons and the amount of enhancement agrees quite well with the theory.

ACKNOWLEDGMENTS

This project was funded by the National Science Foundation Grant no. ECS-8504483, AFOSR 86-0012, and the Michigan Memorial—Phoenix Project of the University of Michigan. The authors wish to acknowledge a valuable discussion with Professor Hans Fleischmann, the technical assistance of Steve Bidwell and Lou Smutek and the valuable comments of Professor Ron Gilgenbach. The authors also acknowledge equipment assistance from the Beam Dynamics Group at the Naval Research Laboratories.

[1]H. A. Koehler, L. J. Ferderber, D. L. Redhead, and P. J. Ebert, Phys. Rev. A **9**, 768 (1973).

[2]P. S. P. Wei, J. L. Adamski, and J. R. Beymer, J. Appl. Phys. **48**, 568 (1977).

[3]J. E. Rizzo, J. Appl. Phys. **40**, 4883 (1969).

[4]D. J. Eckstrom, J. S. Dickinson, and R. M. Hill, J. Chem. Phys. **82**, 1792 (1985).

[5]K. Ono, Jpn. J. Appl. Phys. **18**, 1013 (1979).

[6]C. Rhodes, *Excimer Lasers*, Topics in Applied Physics, Vol. 30 (Springer, New York, 1979).

[7]R. W. Dreyfus and R. T. Hodgson, Appl. Phys. Lett. **20**, 195 (1972).

[8]K. G. Whitney and J. Davis, J. Appl. Phys. **46**, 4103 (1975).

[9]K. Ono, Jpn. J. Appl. Phys. **19**, 1515 (1980).

[10]R. Jayakumar and H. Fleischmann, J. Quant. Spectrosc. Radiat. Transfer **33**, 177 (1985).

[11]E. Lauer, "Universal Curves for Predicting Equilibrium Radii of Relativistic Electron Beams Including the Effect of Attractive Self Force, External B_z, Initial Beam Quality and Scattering in the Gas Entry Foil," UCID-16716, March 1975.

[12]A. Striganov and N. Sventitskii, *Tables of Spectra Lines of Neutral and Ionized Atoms* (IFI/Plenum, New York, 1968).

[13]R. H. Tourin, *Spectroscopic Gas Temperature Measurement* (Elsevier, Amsterdam, 1966), p. 47.

[14]W. Wiese, M. Smith, and B.Glennon, *Atomic Transition Probabilities, Vol. II*, National Standard Reference Data Series, Number 22 (National Bureau of Standards, 1969).

[15]J. Rizzo, J. Appl. Phys. **41**, 4941 (1970).

[16]D. Book, *NRL Plasma Formulary* (Naval Research Laboratory, 1983).

[17]C. Moore, *Atomic Energy Levels: Derived from the Analysis of Optical Spectra*, Circular of NBS no. 467, Department of the National Bureau of Standards (1949).